Numerical simulations for nodal domains and spectral minimal partitions

Virginie Bonnaillie-Noël, Bernard Helffer, Grégory Vial

Numerical simulations for nodal domains and spectral minimal partitions

V. Bonnaillie-Noël*, B. Helffer† and G. Vial*

Abstract

We recall here some theoretical results of B. Helffer, T. Hoffmann-Ostenhof and S. Terracini about minimal partitions and propose numerical computations to illustrate some of their published or unpublished conjectures.

1 Introduction

We are interested in the properties of the "minimal" k-partitions of an open set Ω by k disjoint open sets D_i $(i = 1, \dots, k)$ in Ω. These partitions are minimal in the sense that they minimize the maximum over $i = 1, \dots, k$ of the lowest eigenvalues of the Dirichlet realization of the Laplacian in D_i. Such problems naturally appear in Biomathematics. In particular, we would like to determine in which cases this minimal partition is actually the family of the nodal domains of a given eigenfunction of the two-dimensional Dirichlet Laplacian in Ω. In the case of 2-partitions, the answer is very simple because a variational characterization of the second eigenvalue of the Dirichlet Laplacian in Ω shows that a minimal 2-partition is always a nodal partition corresponding to the second eigenvalue. So the interesting questions start with $k = 3$. Although general properties of these minimal partitions have been proved in [HHOT] by B. Helffer, T. Hoffmann-Ostenhof and S. Terracini (see also [Hel] for a survey – in french), there are very few theoretical results (except for thin rectangles) for obtaining an explicit determination of minimal partitions. This is already the case for 3-partitions and for simple cases like the square or the disk. For these reasons, it is particularly useful to mix some theoretical remarks of [HHOT] and still unpublished results of [HHO2] with efficient numerical computations. This is the main goal of this paper to present these computations and the conjectures which they suggest or numerically confirm.

Acknowledgements
The authors would like thank A. El Soufi, T. Hoffmann-Ostenhof, S. Terracini, M. Van den Berg and G. Verzini for many enlightening and stimulating discussions. The second author was partially supported by the ESF-programme SPECT.

2 Minimal partitions : main definitions

Let Ω be a bounded and regular (i.e. piecewise $C^{1,\alpha}$ for some $\alpha > 0$) connected domain in $\mathbb{R}^2$. The eigenvalues of the Dirichlet realization of the Laplacian $-\Delta$ in Ω are denoted by

*IRMAR, ENS Cachan Bretagne, CNRS, UEB, av Robert Schuman, F-35170 Bruz, France, Virginie.Bonnaillie@bretagne.ens-cachan.fr, Gregory.Vial@bretagne.ens-cachan.fr

†Laboratoire de Mathématiques, Bâtiment 425, Univ Paris-Sud et CNRS, F-91405 Orsay cedex, France, Bernard.Helffer@math.u-psud.fr

$$\lambda_1 < \lambda_2 \leq \lambda_3 \leq ... \leq \lambda_n ...$$

We choose the associated eigenfunctions u_n ($n \in \mathbb{N}^*$) to form an orthonormal basis for $L^2(\Omega)$.
Let $k \geq 1$ be an integer. A *k-weak-partition* (in short "k-partition" or simply "partition") of Ω is a family $\mathcal{D} = (D_i)_{i=1}^k$ of mutually disjoint sets such that

$$\cup_{i=1}^k D_i \subset \Omega.$$

The weak partition is called *open, resp. connected, regular*, if the D_i are open, resp. connected, regular (i.e. piecewise $C^{1,\alpha}$ for some $\alpha > 0$ and with the interior cone condition) sets of Ω. The partition is called *strong* if

$$\mathrm{Int}\,(\overline{\cup_i D_i}) \setminus \partial\Omega = \Omega.$$

The set of open connected weak k-partitions of Ω is denoted by $\mathcal{D}_k(\Omega)$.
For $\mathcal{D} \in \mathcal{D}_k(\Omega)$, we define

$$\Lambda(\mathcal{D}) = \max\{\lambda_1(D_i),\ i = 1, ..., k\},$$

where $\lambda_1(D_i)$ denotes the first eigenvalue[1] of the Dirichlet realization of the Laplacian in D_i.
For any integer $k \geq 1$, we define

$$\mathfrak{L}_k(\Omega) = \inf\{\Lambda(\mathcal{D}),\ \mathcal{D} \in \mathcal{D}_k\}.$$

A weak k-partition $\mathcal{D} \in \mathcal{D}_k(\Omega)$ such that $\Lambda(\mathcal{D}) = \mathfrak{L}_k(\Omega)$ is called *minimal k-partition* of Ω.
Let $u \in C_0^0(\overline{\Omega})$. The *nodal domains* of u (whose number is denoted by $\mu(u)$) are the components of $\Omega \setminus N(u)$ where

$$N(u) = \overline{\{x \in \Omega \mid u(x) = 0\}}.$$

When u is an eigenfunction of the Laplacian, $N(u)$ is a C^∞ curve, except at some isolated critical points of Ω. In a sufficiently small neighborhood of one critical point $x_c \in \Omega$, $N(u)$ is a union of an even number of half-curves meeting at x_c, with tangents crossing with equal angles. At the points x_b of $N(u) \cap \partial\Omega$, we have the analogous property that $N(u)$ is locally a union of half-curves ending at x_b with equal angle with the boundary. This will be referred as to **"equal angle meeting property"**.

3 Main results about minimal partitions

We briefly recall in this section the main results obtained in [HHOT] and emphasize specific results which motivate the strategy used for the numerical computations.

The first result obtained in [HHOT] is that

Theorem 3.1
A minimal partition has always a "strong" representative[2] which is regular.

[1] Note that this can be defined in some extended sense for any open set.
[2] modulo sets of capacity 0.

So the subtilities about weak and strong partitions do not play a role in our numerical computations as soon as we are concerned with minimal partitions. The existence of such minimal partitions was obtained previously in [CTV1, CTV2, CTV3] (see also an earlier contribution giving a weaker result of [BBH]). It has been shown in [HHOT] that the minimal partitions share with the nodal sets many properties. In particular they satisfy the equal angle meeting property but note that the number of half-curves meeting at a critical point may now be odd.

We recall that minimal 2-partitions of Ω are actually nodal partitions associated with some eigenfunction in the eigenspace corresponding to the second eigenvalue $\lambda_2(\Omega)$ of the Dirichlet realization of $-\Delta$ in Ω:

$$\mathfrak{L}_2(\Omega) = \lambda_2(\Omega) \ ,$$

which can be understood as a kind of variational characterization of the second eigenvalue.

We naturally wonder whether this result extends for $k \geq 3$: does any minimal partition correspond to a nodal partition induced by an eigenfunction ?

Two subdomains D_i, D_j are said to be neighbors ($D_i \sim D_j$) if $\mathrm{Int}\,(\overline{D_i \cup D_j}) \setminus \partial\Omega$ is connected.
To each $\mathcal{D}$ corresponds a graph $G(\mathcal{D})$ obtained by associating a vertex to each D_i and an edge to each pair $D_i \sim D_j$. This graph is undirected without multiple edges or loops. It is said *bipartite* if it can be colored by two colors (two neighbours having distinct color). It is well known that nodal partitions are bipartite. The following converse is deeper (see [HHO1], [CTV1, CTV2, CTV3] and [HHOT]) :

Theorem 3.2
If the graph of the minimal partition is bipartite, this is the nodal partition of an eigenfunction corresponding to $\mathfrak{L}_k(\Omega)$.

Theorem 3.3 (Courant's Nodal Theorem)
Let $k \geq 1$, $\lambda_k(\Omega)$ be the $k-$th eigenvalue and u any real eigenfunction of $-\Delta$ on Ω (so that $-\Delta u = \lambda_k u$). Then the number of nodal domains $\mu(u)$ of u satisfies

$$\mu(u) \leq k.$$

If $\mu(u) = k$, we say that u is *Courant-sharp*.

For any integer $k \geq 1$, we denote by L_k the smallest eigenvalue whose eigenspace contains an eigenfunction with k nodal domains. In general, we have the first comparison

Theorem 3.4
Let Ω be a regular open set in $\mathbb{R}^2$, then, for any $k \in \mathbb{N}^*$, we have

$$\lambda_k(\Omega) \leq \mathfrak{L}_k(\Omega) \leq L_k(\Omega) \ . \tag{1}$$

The classical Pleijel Theorem says that $\lambda_k(\Omega) < L_k(\Omega)$ for k large. In other words, an eigenfunction cannot be Courant-sharp for k large.

An improved version of Pleijel's Theorem (which implies this theorem) says :

Theorem 3.5 (Pleijel's Theorem for minimal partitions)
Let Ω be a regular open set in $\mathbb{R}^2$, then there exists k_0 such that, for $k \geq k_0$, we have

$$\lambda_k(\Omega) < \mathfrak{L}_k(\Omega) \ .$$

This in particularly says that a minimal partition can not be nodal for k large. The proof of this result (see [HHOT]) is based on the Faber-Krahn Inequality together with the Weyl Formula.

It is interesting to determine the equality cases. It is fulfilled for $k = 1$ and $k = 2$, it is a mere consequence of the sign properties of the first two eigenfunctions. So the interesting question starts with $k = 3$. It is not too difficult to see that for the square and the disk, the two inequalities are strict and that on the contrary, we have again equality for $k = 4$.

Theorem 3.6
We assume that Ω is regular. If $\mathfrak{L}_k(\Omega) = L_k(\Omega)$ or if $\mathfrak{L}_k(\Omega) = \lambda_k(\Omega)$, then

$$\lambda_k(\Omega) = \mathfrak{L}_k(\Omega) = L_k(\Omega) .$$

Furthermore, there exists in this case an eigenfunction u_k in the eigenspace associated to λ_k such that $\mu(u_k) = k$ (i.e. u_k is Courant-sharp).

In other words, the only case when a minimal partition is a nodal partition is the case when this nodal partition corresponds to a Courant-sharp case.

Let us close this short presentation of minimal partitions by a monotonicity property :

Proposition 3.7
If $\Omega \subset \widehat{\Omega}$, then

$$\mathfrak{L}_k(\widehat{\Omega}) \leq \mathfrak{L}_k(\Omega) . \tag{2}$$

Here it is important to notice that a strong partition of Ω is a weak partition of $\widehat{\Omega}$.

4 Necessary conditions for minimal partitions

It is not straightforward to find a good algorithm for determining numerically[3] minimal partitions. So it is interesting to look for necessary conditions which are easier to analyze.

A first necessary condition is that :

Proposition 4.1
Let $k \geq 3$ and $\mathcal{D} = (D_1, \ldots, D_k)$ a minimal k-partition of Ω. Then, for any pair of neighbours $D_i \sim D_j$, $\mathfrak{L}_k(\Omega)$ should be the second eigenvalue of the Dirichlet Laplacian of[4]

$$D_{ij} = \mathrm{Int}\left(\overline{D_i} \cup \overline{D_j}\right) ,$$

D_i and D_j being the nodal sets of some corresponding eigenfunction.

This is actually a particular case of the more general result which concerns any connected subpartition :

Theorem 4.2
Let $\mathcal{D}$ be a minimal k-partition of Ω relative to $\mathfrak{L}_k(\Omega)$. Let $\Omega' \subset \Omega$ be connected and $\mathcal{D}' \subset \mathcal{D}$ be any subpartition of $\mathcal{D}$ into k' elements ($1 \leq k' < k$) such that

$$\overline{\Omega'} = \cup\{\overline{D_i},\ D_i \in \mathcal{D}'\} .$$

Then $\mathfrak{L}_k(\Omega) = \mathfrak{L}_{k'}(\Omega')$ and this last equality is uniquely achieved.

[3] See however what can be done by using the associated variational problem appearing in the proof of Conti-Terracini-Verzini, or evolutionary algorithms, see [Lan].

[4] Here we recall that, for a given set U in $\mathbb{R}^2$, $\mathrm{Int}\, U$ denotes the interior of U, i.e. the largest open set contained in U.

So any subpartition should be minimal and, implementing previous other results, we also see that

Corollary 4.3
With the assumptions of Theorem 4.2, any subpartition with corresponding bipartite subgraph is a nodal partition. Moreover, it corresponds then to a Courant-sharp situation:

$$\mathfrak{L}_{k'}(\Omega') = \lambda_{k'}(\Omega') \ .$$

In the paper [HHOT], there is also implicitly another interesting necessary condition extending the previous theorem. Starting from a minimal regular k-partition $\mathcal{D}$ of a domain Ω, we can construct in Ω a connected domain $\widetilde{\Omega}$ such that $\mathcal{D}$ becomes a minimal k-bipartite partition of $\widetilde{\Omega}$. It is achieved by removing from Ω a union of a finite number of regular arcs corresponding to pieces of boundaries between two neighbours of the partition. Note that this construction can be done in many ways. For an example, see Figure 21. We say in this case that $\widetilde{\Omega}$ is an extracted open set associated to $\mathcal{D}$. As second corollary, we obtain

Corollary 4.4
If $\mathcal{D}$ is a minimal regular k-partition, then for any extracted connected open set $\widetilde{\Omega}$ associated with $\mathcal{D}$, we have

$$\lambda_k(\widetilde{\Omega}) = \mathfrak{L}_k(\widetilde{\Omega}) \ . \tag{3}$$

This last criterion will be analyzed below for union of triangles, squares and hexagons as a test of minimality. The numerical computations will show a quite different behavior, which in the two first cases was expected by the theory as we will see in Subsection 6.5.

5 Minimal partitions and symmetries

5.1 Topological configurations

If the domain has symmetries, it is natural to wonder whether the symmetry properties are reflected in the properties of the minimal partitions. Symmetry properties of the partition allow simplification in the analysis of the possible candidates for a minimal partition. Under this assumption, we can hope to find at least a good strategy for doing numerics.

This will be done in this article in the case of 3-partitions. We assume that the domain Ω has a symmetry σ with respect to some axis (hence $\sigma^2 = Id$)

$$\sigma(\Omega) = \Omega \ , \tag{4}$$

and that, instead of minimizing over all the partitions, we only minimize over the "symmetric" partitions, i.e. partitions which satisfy either

$$\sigma(D_i) = D_i \ , \quad \text{for } i = 1, \dots 3 \ , \tag{5}$$

or (after a possible relabelling)

$$\sigma(D_1) = D_2 \ , \ \sigma(D_3) = D_3 \ . \tag{6}$$

The proof giving the existence of a minimal partition goes through in the symmetric case (i.e. when we minimize over 3-partitions satisfying (6)) and so it is natural to look for a symmetric minimizer.

Let us add two notions attached to a strong regular open partition. We call *critical point* a point which lies at the intersection of the boundaries of at least three open sets

of the partition. We call *boundary point* a point at the intersection of the boundary of Ω with at least the boundaries of two open sets of the partition. In the example of Figure 5, x_0 is a critical point and a is a boundary point.

It follows from the Euler formula (see [HHO2]) that these minimizers can be classified: we separate bipartite 3-partitions and non bipartitie ones and for each case, we give an exhaustive list of possible configurations.

Bipartite 3-partition

A first possibility is that the minimal 3-partition is bipartite (hence a nodal domain). The most natural case is illustrated in Figure 1. In the situation of Figure 1, the minimal

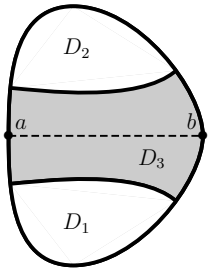

Figure 1: The 3-partition has no critical point.

3-partition corresponds to the third nodal partition of Ω. This case effectively occurs for a thin vertical rectangle. For general Ω's, numerics can help to determine if the third eigenfunction is Courant-sharp. Beside this situation, there are many other possibilities which can not be excluded a priori :

- 3-partitions with no critical point: this structure brings into play two disjoint "circles"[5] (this provides two configurations: the first one with disjoint "disks" corresponding to the circles, the second one with one "circle" inside the "disk" of the other, see Figures 2);

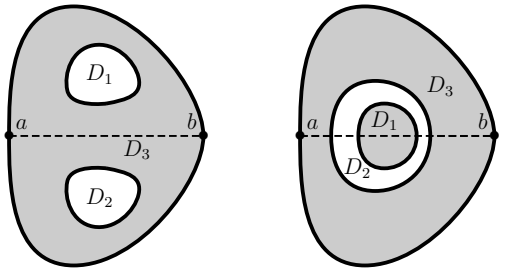

Figure 2: The 3-partition has two disjoint circles.

- 3-partitions with two boundary points (see Figures 3) which can be described with one "circle" and one "line" joining two points of the boundary;
- 3-partitions with one *double point* (see Figures 4) which can be gathered in topological sets: a closed line with a double point and with D_1 and D_2 on both sides or one

[5] A "circle" is simply a closed curve without critical point.

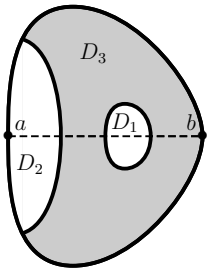

Figure 3: The 3-partition has one circle and one line.

inside the other, or a line joining two points of the boundary but with a double point.

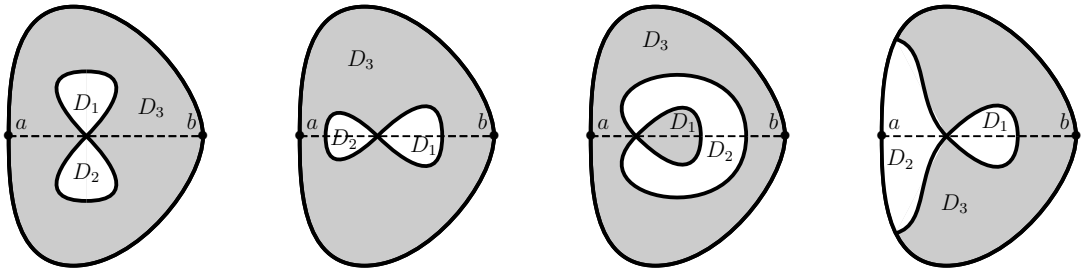

Figure 4: The 3-partition has one double point.

Any configuration previously quoted above for the bipartite 3-partition can be achieved numerically if there exists. All we need is to compute the third eigenfunction and to determine its nodal domains. If the third eigenfunction is Courant-sharp, it provides such a bipartite 3-partition.

Non bipartite 3-partition
The second possibility is the case when the minimal partition is not bipartite. We can only have one of the three following structures whose topology is illustrated in Figures 5, 6, 7.

(a). The 3-partition has one critical point, which is necessarily on the symmetry axis (cf. Figure 5).

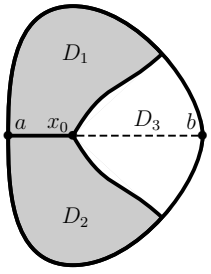

Figure 5: The 3-partition has one critical point.

(b). The 3-partition has two critical points and no boundary point (cf. Figure 6).

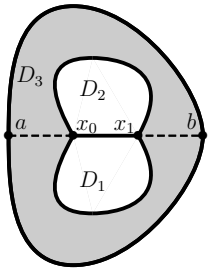

Figure 6: The 3-partition has two critical points and no boundary point.

(c). The 3-partition has two critical points and two boundary points. Moreover $\partial D_1 \cap \partial D_2$ consists of two segments on the symmetry axis, each one joining one boundary point to one critical point (cf. Figure 7).

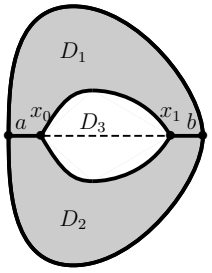

Figure 7: The 3-partition has two critical points and two boundary points.

We now assume that the minimal 3-partition is not bipartite. We want to investigate numerically if one of the previous configurations provides a good candidate for being a minimal symmetric 3-partition. For this purpose, we deal with each case separately.

5.2 Case (a)

Let us define the notations illustrated in Figure 5. We assume that the symmetry axis is $y = 0$ in $\mathbb{R}^2_{x,y}$ and we denote by x_0 the critical point. We assume that Ω is convex to simplify the discussion and denote by (a, b) the segment $\Omega \cap \{y = 0\}$. Without loss of generality, we may assume that $\partial D_1 \cap \partial D_2$ is the segment $[a, x_0]$ and that $\partial D_1 \cap \partial D_3$ consists of a line joining (without any selfintersection) x_0 to $\partial\Omega \cap \{y > 0\}$.
If $\mathcal{D} = (D_1, D_2, D_3)$ is a minimal partition of type (a), then (D_1, D_3) is a minimal 2-partition and hence the nodal partition associated with the second eigenvalue of $D_{13} = \mathrm{Int}\,(\overline{D_1} \cup \overline{D_3})$ (cf. Corollary 4.3). Restricting the corresponding eigenfunction to $\Omega^+ = \Omega \cap \{y > 0\}$, we obtain an eigenfunction φ of the mixed Dirichlet-Neumann problem illustrated in Figure 8:

$$-\Delta\varphi = \lambda\varphi \text{ in } \Omega^+, \quad \partial_{\mathbf{n}}\varphi = 0 \text{ on } [x_0, b] \quad \text{and} \quad \varphi = 0 \text{ elsewhere on the boundary.}$$

Note that we can not ensure that φ is the second eigenfunction of the mixed problem.

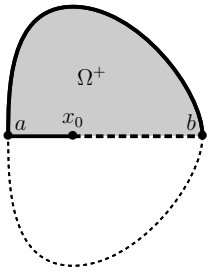

Figure 8: Dirichlet-Neumann problem.

We focus on the second eigenmode $(\lambda_2(x_0), \varphi_{x_0})$ of the mixed problem (see Remark 5.1 for the following ones). Hopefully φ_{x_0} has a nodal line starting from (a, b) and reaching another part of the boundary $\partial\Omega^+ \cap \{y > 0\}$[6]. The following remarks settle our strategy:

- The mapping $x_0 \mapsto \lambda_2(x_0)$ is an increasing function.
- After symmetrization, a nodal line joining (x_0, b) to a point of $\partial\Omega^+ \cap \{y > 0\}$ leads only to a 2-partition of Ω.
- If the nodal line starts from $\xi \in (a, x_0)$, the 3-partition obtained after symmetrization may be improved by removing the segment (ξ, x_0).

Altogether, moving x_0 along the segment $[a, b]$, we expect the second eigenfunction to have a nodal line joining x_0 to the boundary $\partial\Omega \cap \{y > 0\}$. The smallest x_0 corresponding to this configuration (if there exists) is denoted by x_0^*. The eigenvalue $\lambda_2(x_0^*)$ provides an upper bound of $\mathfrak{L}_3(\Omega)$ and the nodal domains of the associated eigenfunction $\varphi_{x_0^*}$ give a possible candidate for the minimal 3-partition of Ω.

From the equal angle meeting property, we know that the nodal line joining x_0^* to the boundary $\partial\Omega \cap \{y > 0\}$ and the segment $[a, x_0^*]$ meet at x_0^* with an angle of $2\pi/3$. If $x_0 \neq x_0^*$, then the nodal line is orthogonal to $[a, b]$ since, after symmetrization, the point x_0 is the intersection point of two half-curves if $a < x_0 < x_0^*$ (the nodal line joining x_0 to the boundary $\partial\Omega \cap \{y > 0\}$ and its symmetric line) or four half-curves if $x_0^* < x_0 < b$ ($[a, \xi]$, $[\xi, x_0]$, the nodal line starting from ξ and its symmetric).
Let z_0^+ be the intersection point between the boundary $\partial\Omega \cap \{y > 0\}$ and the nodal line joining x_0^* to $\partial\Omega \cap \{y > 0\}$. If the boundary $\partial\Omega \cap \{y > 0\}$ is smooth at z_0^+, then the nodal line is orthogonal to the boundary at z_0^+. If z_0^+ is a vertex of Ω, then, locally around z_0^+, the nodal line splits the domain Ω in two domains with equal angles at z_0^+.

We now present results for several simple shapes: the square, the disk, and the union of three touching hexagons. The computations (see [BV]) have been made with the Finite Element Library MÉLINA [Melina] using 6-order triangular elements, leading to accurate values (with relative error smaller than 0.01%). More computations are available on the web page

http://www.bretagne.ens-cachan.fr/math/simulations/MinimalPartitions/form2.php

[6]This question refers to the nodal line conjecture but the Melas [Mel] Theorem about the non existence closed nodal line is only proved in the convex case with Dirichlet conditions.

Example 1: the square

It turns out that for $x_0 < (a+b)/2$, the second eigenmode only generates a 2-partition of Ω. Moreover for $x_0 = (a+b)/2$, the nodal line joins x_0 to the top boundary. Hence $x_0^* = (a+b)/2$. Let us mention that for $x_0 > x_0^*$, the nodal line starts from $\xi \in (a, x_0)$. Figures 9 illustrate these three cases. These figures illustrate also the equal angle meeting property. We first observe that the nodal line joining x_0 to the boundary $\partial\Omega \cap \{y > 0\}$ is orthogonal to $\partial\Omega \cap \{y > 0\}$. Secondly, the nodal line is orthogonal to (a, x_0) if x_0 is different from x_0^* and the angle between these two curves equals $2\pi/3$ when $x_0 = x_0^*$.

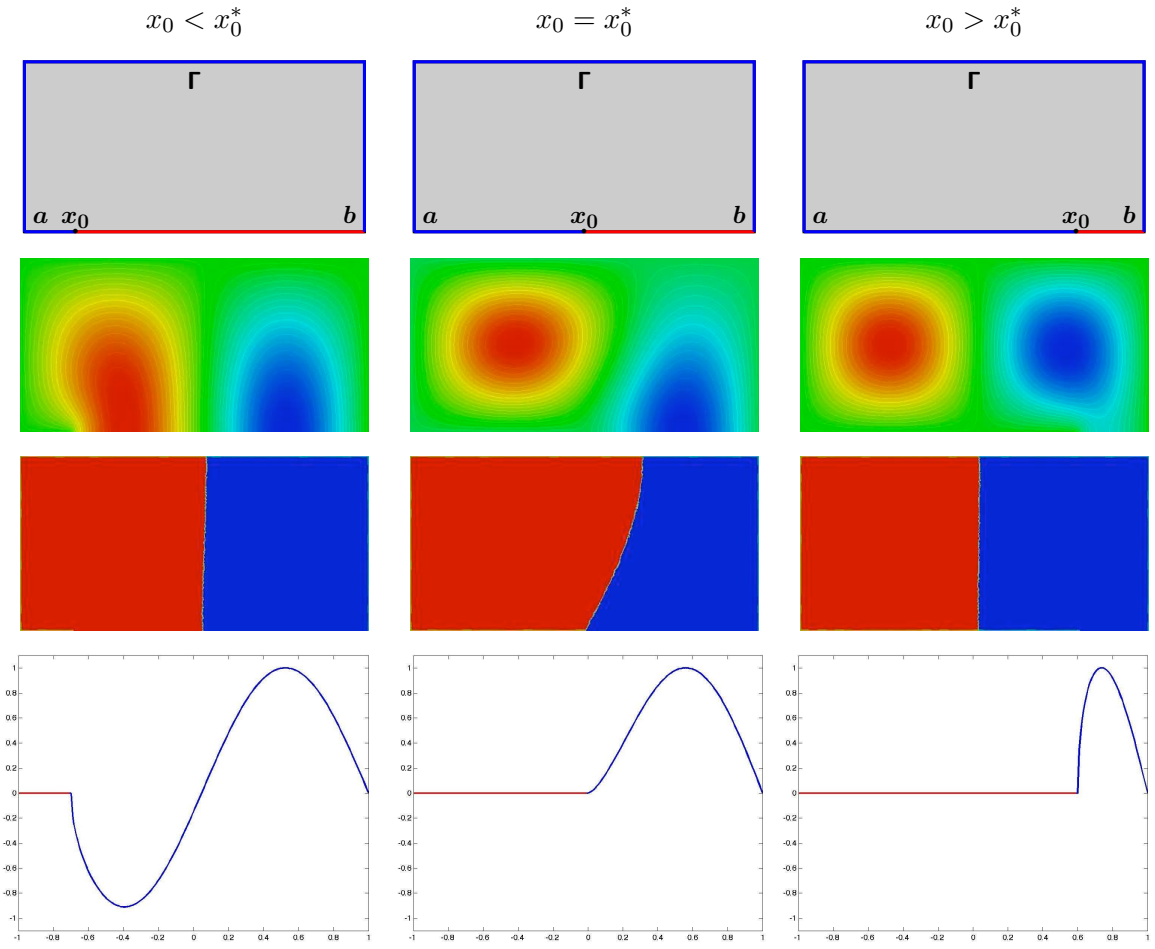

Figure 9: Eigenfunctions for the Dirichlet-Neumann problem on the half-square. *First row: the domain, Second row: the second eigenfunction* φ_{x_0}*, Third row: the nodal domains of* φ_{x_0}*, Fourth row: trace of* φ_{x_0} *on* $y = 0$.

Example 2: the disk

We recover the natural candidate (straight segment) for the disk, with x_0^* at the center of the disk. The possible minimal 3-partition seems to be the family consisting of three identical sectors (see Figure 10). The properties about the angle between the nodal line and the boundary $\partial\Omega \cap \{y > 0\}$ or the line (a, x_0) are the same than in the case of the square.

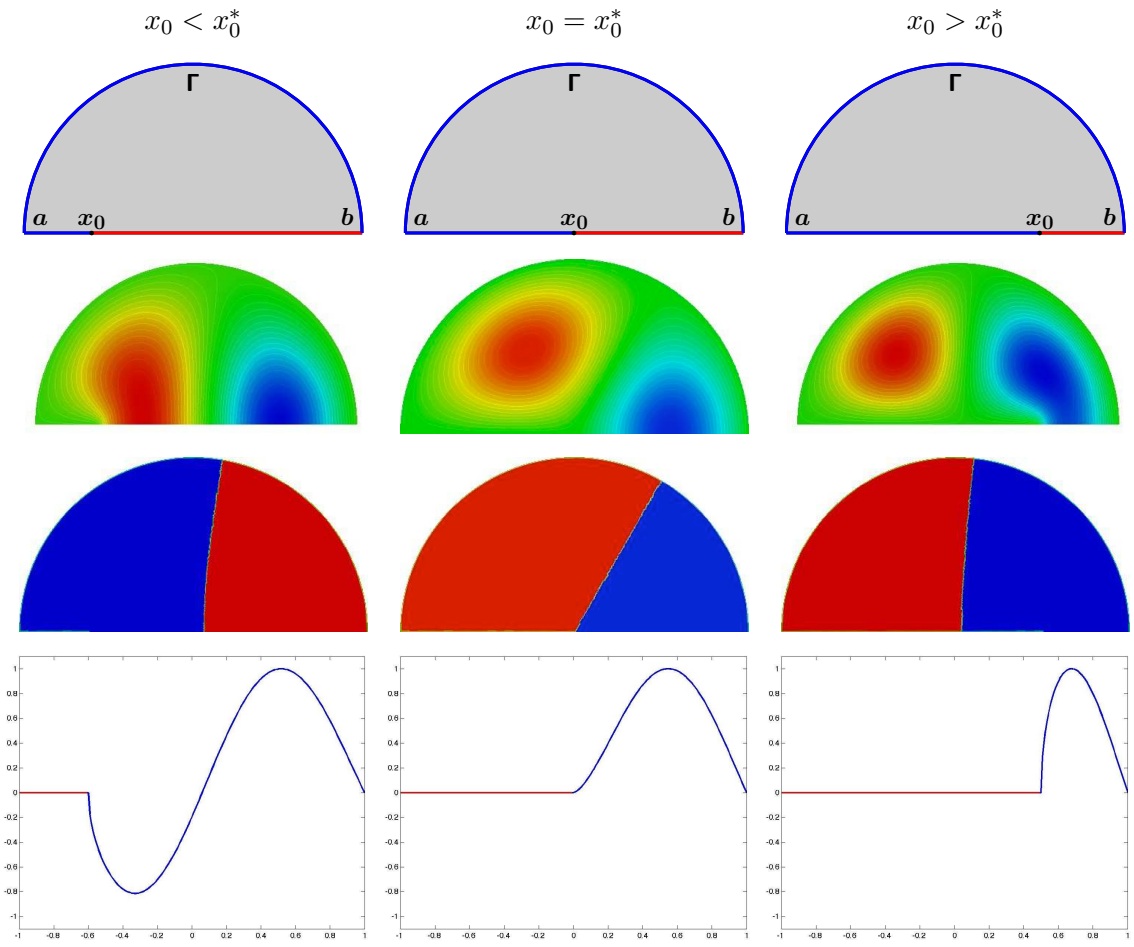

Figure 10: Eigenfunctions for the Dirichlet-Neumann problem on the half-disk. *First row: the domain, Second row: the second eigenfunction* φ_{x_0}*, Third row: the nodal domains of* φ_{x_0}*, Fourth row: trace of* φ_{x_0} *on* $y = 0$.

Example 3: the union of three touching hexagons
The configuration built from $\varphi_{x_0^*}$ after symmetrization corresponds to the three hexagons composing the domain (see Figure 11). Looking at Figures 11, we notice that the nodal line is orthogonal to the boundary $\partial\Omega \cap \{y > 0\}$ as soon as $x_0 \neq x_0^*$ and the angle between these two curves equals $2\pi/3$ when $x_0 = x_0^*$.

Remark 5.1
One cannot exclude a priori that the third (or further) eigenmode for some x_0 *will provide a better configuration than* $(\lambda_2(x_0^*), \varphi_{x_0^*})$*. However, we know that* $\lambda_3(x_0) \geq \lambda_3(a)$ *for any* $x_0 \in [a, b]$*, and in the three samples tested previously, computations show that* $\lambda_3(a) > \lambda_2(x_0^*)$ *(see Table 1). Consequently, only the second eigenmode can generate an interesting candidate.*

5.3 Cases (b) and (c)

The analysis of the last two cases can be done similarly. This time we get a Dirichlet-Neumann-Dirichlet or Neumann-Dirichlet-Neumann condition on $[a, b]$ (see Figure 12). We denote respectively by $\lambda_k^{DND}(x_0, x_1)$ and $\lambda_k^{NDN}(x_0, x_1)$ the k-th eigenvalues of the mixed

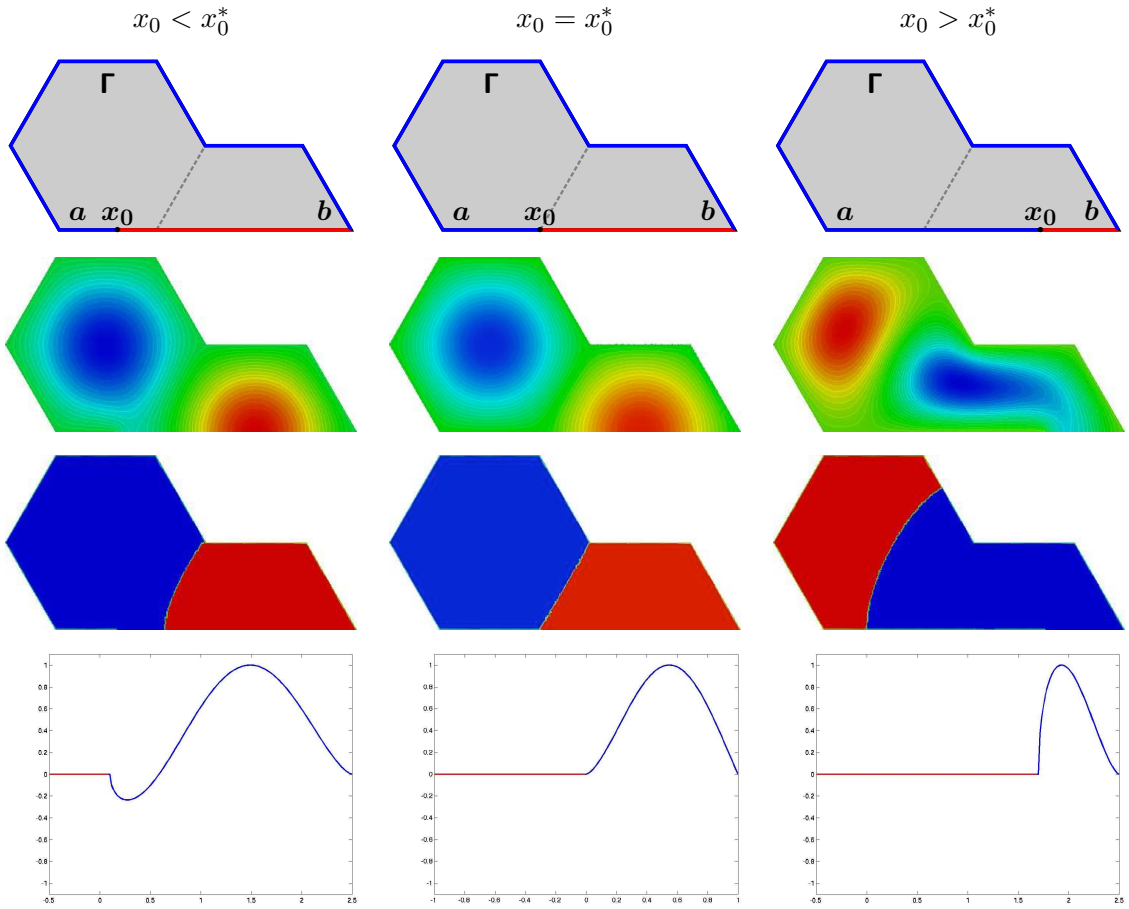

Figure 11: Eigenfunctions for the Dirichlet-Neumann problem on the half-three hexagons. *First row: the domain, Second row: the second eigenfunction* φ_{x_0}*, Third row: the nodal domains of* φ_{x_0}*, Furth row: trace of* φ_{x_0} *on* $y = 0$.

	x_0^*	$\lambda_2(x_0^*)$	$\lambda_3(a)$
Square	$(a+b)/2$	16.6453	24.6740
Disk	$(a+b)/2$	20.1994	26.3860
3-hexagons	$(a+b)/3$	18.5901	27.5868

Table 1: Numerical eigenvalues for the square, the disk and the 3-hexagons.

problem with Neumann conditions respectively on $[x_0, x_1]$ and $[a, x_0] \cup [x_1, b]$ and Dirichlet conditions elsewhere (cf. Figure 12). Obvisously, we have

$$\lambda_k^{DND}(x_0, x_1) \geq \lambda_k(x_0) \geq \lambda_k(a) \qquad \text{and} \qquad \lambda_k^{NDN}(x_0, x_1) \geq \lambda_k(a). \tag{7}$$

As in the case of the Dirichlet-Neumann condition, we compute the second eigenmode but numerical computations for the semi-square, the semi-disk and the semi-3-hexagon suggest that the nodal line of the second eigenfunction never creates a 2-partition of Ω^+ leading by symmetry to a 3-partition of Ω. Figures 13 and 14 give the eigenfunction associated with $\lambda_2^{DND}(x_0, x_1)$ and $\lambda_2^{NDN}(x_0, x_1)$ respectively. Changing the parameters x_0 and x_1 do not change the configuration. We can look at the following modes to generate a better

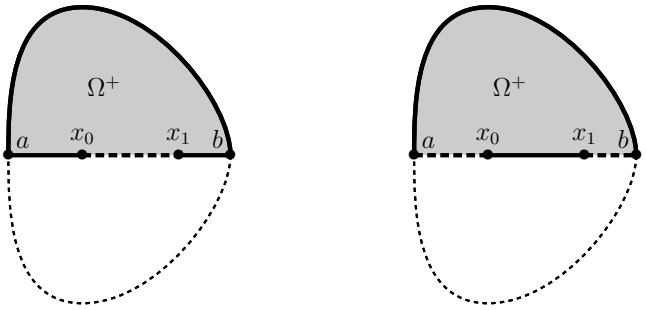

Figure 12: Dirichlet-Neumann-Dirichlet or Neumann-Dirichlet-Neumann problem.

candidate for a 3-partition. As mentionned in (7), the third eigenvalue is always bounded from below by $\lambda_3(a)$. In the case of the square, the disk and the 3-hexagon, numerical estimates given in Table 1 show that $\lambda_3(a)$ is larger than $\lambda_2(x_0^*)$, the best "energy" obtained by the mixed problem Dirichlet-Neumann. Then, the only symmetric candidate is given by the Dirichlet-Neumann condition.

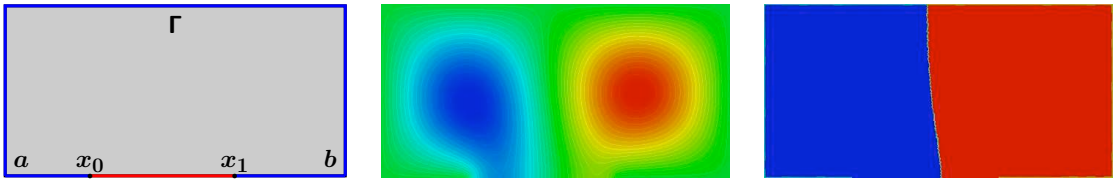

Figure 13: Eigenfunctions for the Dirichlet-Neumann-Dirichlet problem on the half-square.
Left: the domain, Center: the second eigenfunction, Right: the associated nodal domains.

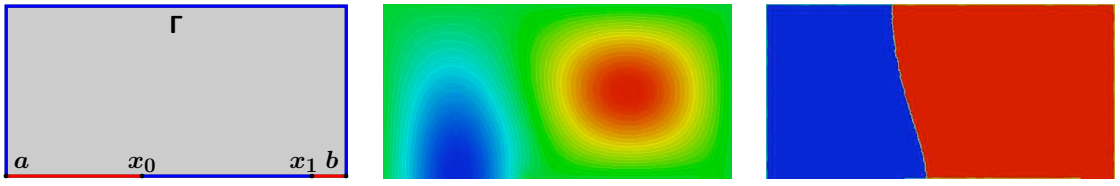

Figure 14: Eigenmodes for the Neumann-Dirichlet-Neumann problem on the half-square.
Left: the domain, Center: the second eigenfunction, Right: the associated nodal domains.

6 On the asymptotic behavior of $\mathfrak{L}_k(\Omega)/k$

6.1 Introduction

An interesting question was communicated to the authors of [HHOT] by M. Van den Berg. We would like also to thank A. El Soufi for discussions around this problem. By the Faber-Krahn Inequality it is easy to see that

$$\lambda_1(Disk_1) \leq |\Omega| \frac{\mathfrak{L}_k(\Omega)}{k} , \tag{8}$$

where $Disk_1$ is the disk of area 1.
On the other hand, if one considers any tiling associated with a discrete group of isometries[7] of $\mathbb{R}^2$ and if D_1 is the fundamental cell (which could be a square, a triangle or an hexagon), then we have asymptotically the upper bound

$$|\Omega| \limsup_{k\to+\infty} \frac{\mathfrak{L}_k(\Omega)}{k} \leq |D_1|\lambda_1(D_1) \ . \tag{9}$$

Here are a few numerical (sometimes exact) values corresponding to the $Hexa_1$, T_1, and Sq_1 being respectively a regular hexagon, an equilateral triangle and a square of area 1. Then

$$\lambda_1(Hexa_1) \sim 18.5901 \ , \ \lambda_1(Sq_1) = 2\pi^2 \sim 19.7392 \ , \ \lambda_1(T_1) \sim 22.7929. \tag{10}$$

Then, as it is well known, we observe that the lowest eigenvalue of the Dirichlet realization of the Laplacian on the regular hexagon of area 1 is lower than the ground state energy of the triangle or the square of same area.

Beside the ground state energy of the disk is

$$\lambda_1(Disk_1) \sim 18.1695 \ . \tag{11}$$

So we get

$$\lambda_1(Disk_1) \leq |\Omega| \liminf_{k\to+\infty} \frac{\mathfrak{L}_k(\Omega)}{k} \ \leq |\Omega| \limsup_{k\to+\infty} \frac{\mathfrak{L}_k(\Omega)}{k} \leq \lambda_1(Hexa_1) \ , \tag{12}$$

with

$$\lambda_1(Disk_1) < \lambda_1(Hexa_1) \ . \tag{13}$$

This leads to two conjectures.

Conjecture 6.1
The limit of $\mathfrak{L}_k(\Omega)/k$ as $k \to +\infty$ exists.

Actually this limit might be more explicit:

Conjecture 6.2

$$|\Omega| \lim_{k\to+\infty} \frac{\mathfrak{L}_k(\Omega)}{k} = \lambda_1(Hexa_1) \ .$$

This last conjecture says in particular that the limit is independent of Ω if Ω is a regular domain.

Of course the optimality of the regular hexagonal tiling appears in various contexts in Physics. But we have at the moment no idea of any approach for proving this in our context. We will explore only numerically why this conjecture looks reasonable.

Remark 6.3
The following argument shows that tiling with hexagons is better than with disks. Looking at Figure 15, tiling with disks generates holes in the domain. Let us give the area of these holes. Let R be the radius of the considered disk. Then the area of a hole $\mathcal{A}(R)$ is equal

[7] We say that a strong partition $\mathcal{D} = (D_i)_{i\geq 1}$ of $\mathbb{R}^2$ is a tiling (in french "pavage") of $\mathbb{R}^2$ associated with Γ if Γ is a discrete group of isometries such that for any $D_i \in \mathcal{D}$, there exists $\gamma \in \Gamma$ with $D_i = \gamma D_1$, and such that $\gamma D_1 = \gamma' D_1$ implies $\gamma = \gamma'$.

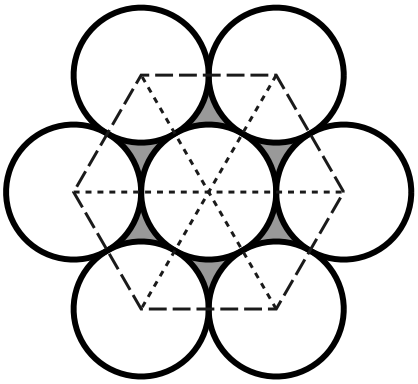

Figure 15: Tiling with disks.

to the difference between the area of an equilateral triangle $\mathcal{A}_T(R)$ *of side* $2R$ *and the half area of a disk* $\mathcal{A}_D(R)$ *of radius* R*. We compute easily that*

$$\mathcal{A}_T(R) = R^2\sqrt{3} \qquad \textit{and} \qquad \mathcal{A}_D(R) = \pi R^2.$$

Then

$$\mathcal{A}(R) = \mathcal{A}_T(R) - \frac{1}{2}\mathcal{A}_D(R) = R^2\left(\sqrt{3} - \frac{\pi}{2}\right).$$

If we consider a disk of area one, then $R = 1/\sqrt{\pi}$ *and then*

$$\mathcal{A}\left(\frac{1}{\sqrt{\pi}}\right) = \frac{\sqrt{3}}{\pi} - \frac{1}{2} \simeq 5.1329 \times 10^{-2}.$$

The area of the hexagon drawn in Figure 15 equals $6\sqrt{3}/\pi$ *and the area of the pieces of disks inside this hexagon equals* 3*. Then, we have to compare*

$$\frac{\lambda_1(Disk_1)}{3} \times \frac{6\sqrt{3}}{\pi} = \frac{2\sqrt{3}}{\pi}\lambda_1(Disk_1) \simeq 20.0347 \qquad \textit{and} \qquad \lambda_1(Hexa_1) \simeq 18.5901.$$

It follows that the tiling with regular hexagons gives lower energy than those with disks.

6.2 Towards a definition of uniform minimal partition of $\mathbb{R}^2$

Let us start from an infinite strong regular partition $\mathcal{D}$ of $\mathbb{R}^2$. Of course we are principally interested in tilings attached to a discrete group of isometries Γ but it seems interesting to have a slightly more general notion. One could be interested for example in starting from a tiling and in considering a refined partition obtained by repartitioning each D_i of the tiling and using a minimal m-partition of D_i.
Another possibility could be to create a fundamental "molecule" $\mathcal{M}_0$ by gluing together a union of m previous D_i, and then considering a new m-partition of this molecule.

To cover all these cases, we are led to introduce a notion of uniformity. We introduce an open partition $\mathcal{D} = (D_i)_{i\in I}$, covering $\mathbb{R}^2$:

$$D_i \cap D_j = \emptyset \text{ if } i \neq j \ , \tag{14}$$

and

$$\cup_{i\in I}\overline{D_i} = \mathbb{R}^2 \ . \tag{15}$$

We also assume that each D_i is bounded and that the partition is locally finite in the sense that :

$$\text{Any disk of } \mathbb{R}^2 \text{ is contained in a finite union of } \overline{D_i}\text{'s.} \tag{16}$$

If Ω is a non empty regular bounded open set of finite area $|\Omega|$, let us consider for any $R > 0$ the dilated $\delta_R\Omega$ (by the map $x \mapsto Rx$) and two subsets of I : $I^{int}(R,\Omega)$ and $I^{ext}(R,\Omega)$, defined by

$$I^{int}(R,\Omega) = \{i \in I \mid D_i \subset \delta_R\Omega\} \ , \tag{17}$$

and

$$I^{ext}(R,\Omega) = I^{int}(R,\Omega) \cup I^{bnd}(R,\Omega) \ , \tag{18}$$

where

$$I^{bnd}(R,\Omega) = \{i \in I \mid \partial\delta_R\Omega \cap D_i \neq \emptyset\}. \tag{19}$$

By (16) it is clear that

$$\#I^{ext}(R,\Omega) < +\infty \ , \tag{20}$$

for any bounded regular Ω.

Remark 6.4
Note that in the case of a tiling, one has the following properties

$$\#I^{int}(R,\Omega) \sim R^2 \frac{|\Omega|}{|D_1|} \ , \tag{21}$$

and

$$\#I^{bnd}(R,\Omega) = \mathcal{O}(R) \ . \tag{22}$$

The question is then to define a reasonable notion of uniform minimal $\mathbb{R}^2$-partition. A possible definition could be :

Definition 6.5
An infinite strong regular uniform partition $\mathcal{D}$ of $\mathbb{R}^2$ is called a minimal $\mathbb{R}^2$-partition *if, for any k, any connected subpartition $(D_i)_{i\in I}$ of cardinal $k = |I|$ is a minimal k-partition of $D_I = \mathrm{Int}\,(\cup_i \overline{D_i})$.*

We did not know if such partitions exist but they seem to be rather good candidates for an accurate upper bound in the problem above.

Remark 6.6
Note that any open set D_i of the minimal $\mathbb{R}^2$-partition has by definition the same ground-state $\lambda_1(D_i)$.

We now want to estimate $\mathfrak{L}_k(\Omega)$ using the dilations δ_R.

6.3 Upper bounds

Given a $\mathbb{R}^2$-partition $\mathcal{D}$ satisfying (14), (15), (16) and

$$\lambda_1(D_i) = \lambda_1(D_j) \ , \ \forall i, j \ , \tag{23}$$

we start from

$$\mathfrak{L}_k(\Omega) = R^2 \mathfrak{L}_k(\delta_R \Omega) \ . \tag{24}$$

Now if R satisfies

$$\#I^{int}(R, \Omega) \geq k \ , \tag{25}$$

we obtain

$$\mathfrak{L}_k(\Omega) \leq R^2 \lambda_1(D_i) \ . \tag{26}$$

The optimal $R^{int}(k, \Omega)$ is given by

$$R^{int}(k, \Omega) := \inf\{R \mid \#I^{int}(R, \Omega) \geq k\} \ . \tag{27}$$

Note that $k \mapsto R^{int}(k, \Omega)$ is monotonically increasing.
So we get the upper bound

$$\frac{\mathfrak{L}_k(\Omega)}{k} \leq \frac{R^{int}(k, \Omega)^2}{k} \lambda_1(D_i) \ . \tag{28}$$

Passing to the limit, we obtain

$$\limsup_{k \to +\infty} \frac{\mathfrak{L}_k(\Omega)}{k} \leq \limsup_{k \to +\infty} \frac{R^{int}(k, \Omega)^2}{k} \ \lambda_1(D_i) \ . \tag{29}$$

We can define

$$\overline{\mathfrak{L}_\infty}(\mathcal{D}, \Omega) := |\Omega| \limsup_{k \to +\infty} \frac{R^{int}(k, \Omega)^2}{k} \ \lambda_1(D_i) \ . \tag{30}$$

Remark 6.7
When $\mathcal{D}$ is a tiling, then we can obtain that

$$|\Omega| \limsup_{k \to +\infty} \frac{R^{int}(k, \Omega)^2}{k} = |D_1| \ . \tag{31}$$

But this is not the case in full generality, in particular when the D_i have not the same area.

The molecule situation is also interesting to analyze. The partition $\mathcal{D}$ can be relabelled as a family D_{pq} with $p \in J$, and $q = 1, \ldots, m$ where m is the size of the molecule. The family of molecules is here

$$\mathcal{M}_p = \text{Int} \ \left(\cup_{q \in \{1, \ldots, m\}} \overline{D_{pq}} \right) ,$$

and we assume that $\mathcal{M}_p$ is a tiling associated with a discrete group.

In this case we obtain

$$|\Omega| \limsup_{k \to +\infty} \frac{R^{int}(k, \Omega)^2}{k} = \frac{|\mathcal{M}_0|}{m} \ , \tag{32}$$

where $\mathcal{M}_0$ is one of the molecule.

6.4 Lower bounds

Conversely, one can look for lower bound. We consider $\mathcal{D}$, Ω and some k as previously. We define

$$R^{ext}(k,\Omega) = \sup\{R \mid \#I^{ext}(R,\Omega) \leq k\} \ . \tag{33}$$

It is easy to see that $k \mapsto R^{ext}(k,\Omega)$ is increasing and satisfies

$$R^{ext}(k,\Omega) \leq R^{int}(k,\Omega) \ . \tag{34}$$

Let us look at the lower bound. We have, for $R \leq R^{ext}(k,\Omega)$,

$$\mathfrak{L}_k(\Omega) = R^2\mathfrak{L}_k(\delta_R\Omega) \geq R^2\mathfrak{L}_{\#I^{ext}(R,\Omega)}(\mathcal{D}_{I^{ext}(R,\Omega)}) \ . \tag{35}$$

Here we have simply used the domain monotonicity of $\mathfrak{L}_k$.

Since the partition is minimal (This is the first time that we use fully this property!), we observe that

$$\mathfrak{L}_{\#I^{ext}(R,\Omega)}(\mathcal{D}_{I^{ext}(R,\Omega)}) = \lambda_1(D_1) \ .$$

We then obtain

$$\mathfrak{L}_k(\Omega) \geq R^{ext}(k,\Omega)^2\lambda_1(D_1), \tag{36}$$

and consequently

$$\liminf_{k\to+\infty} \frac{\mathfrak{L}_k(\Omega)}{k} \geq \liminf_{k\to+\infty} \frac{R^{ext}(k,\Omega)^2}{k}\lambda_1(D_1) \ . \tag{37}$$

So the weakest notion of regularity of the minimal $\mathbb{R}^2$-partition relatively to Ω and its dilations is the condition that

$$\liminf_{k\to+\infty} \frac{R^{ext}(k,\Omega)^2}{k} = \limsup_{k\to+\infty} \frac{R^{int}(k,\Omega)^2}{k} \tag{38}$$

If the minimal $\mathbb{R}^2$-partition $\mathcal{D}$ is in addition a tiling, then this property is actually true for any regular open set Ω. One has indeed

$$|\Omega| \liminf_{k\to+\infty} \frac{R^{ext}(k,\Omega)^2}{k} = |D_1| = |\Omega| \limsup_{k\to+\infty} \frac{R^{int}(k,\Omega)^2}{k} \ . \tag{39}$$

So we have proved the

Proposition 6.8
Suppose that there exists a minimal $\mathbb{R}^2$-partition $\mathcal{D}$ which is a tiling, then $\mathfrak{L}_k(\Omega)/k$ tends to a limit given by :

$$|\Omega| \lim_{k\to+\infty} \frac{\mathfrak{L}_k(\Omega)}{k} = |D_1|\lambda_1(D_1) \ . \tag{40}$$

Remark 6.9
In particular if we show that the hexagonal tiling is a minimal $\mathbb{R}^2$-partition, we get that $\lambda_1(Hexa_1)$ is effectively the limit of $|\Omega|\mathfrak{L}_k(\Omega)/k$.

6.5 About self-similar tilings

A natural idea is the following: starting from these basic tilings, we try and construct new tilings permitting to improve the upper bound.

Theorem 6.10
A bipartite self-similar tiling is never minimal in the sense of the previous definition.

By self-similar we mean that there exists some integer $m > 1$ such that $\delta_m D_1$ is a union of m^2 open sets of the initial tiling. For example the square is covered by four squares, the equilateral triangle can also be written as the union of four triangles. The regular hexagonal tiling is NOT self-similar.

Proof. Let D_1 be a fundamental cell assumed of area 1. We wonder if there exists an integer $n \geq 1$ such that $\mathfrak{L}_{m^{2n}}(\delta_{m^n} D_1) < \lambda_1(D_1)$. If not, we have for any $n \geq 1$,

$$\mathfrak{L}_{m^{2n}}(\delta_{m^n} D_1) = \lambda_1(D_1). \tag{41}$$

Using the eigenvector associated with $\lambda_1(D_1)$, we can construct an eigenvector with m^{2n} nodal sets for the bipartite domain $\delta_{m^n} D_1$. From (41), it follows that the partition is nodal and hence Courant-Sharp by Theorem 3.6. Then

$$\lambda_1(D_1) = \mathfrak{L}_{m^{2n}}(\delta_{m^n} D_1) = \lambda_{m^{2n}}(\delta_{m^n} D_1)\ .$$

By dilation consideration, we have

$$\lambda_{m^{2n}}(\delta_{m^n} D_1) = \frac{\lambda_{m^{2n}}(D_1)}{m^{2n}}\ .$$

We recall the Weyl's asymptotics (this is the same argument as for Pleijel's Theorem)

$$\lambda_k(\Omega) \sim 4\pi \frac{k}{|\Omega|} \quad \text{as} \quad k \to +\infty.$$

Applying this asymptotics with $k = m^{2n}$ and $\Omega = \delta_{m^n} D_1$, we get

$$\lambda_{m^{2n}}(\delta_{m^n} D_1) \sim 4\pi \frac{m^{2n}}{|\delta_{m^n} D_1|} = 4\pi \quad \text{as} \quad n \to +\infty. \tag{42}$$

This leads to a contradiction since $4\pi < \lambda_1(Disk1) < \lambda_1(D_1)$. □

Remark 6.11
Note that the regular hexagonal tiling is not self-similar.

Let us illustrate Theorem 6.10 with numerical simulations on equilateral triangles and squares. Let T_1 and Sq_1 be respectively an equilateral triangle and a square of area 1. From 4^n patterns T_1 or Sq_1, we construct new equilateral triangles and squares of area 4^n denoted by T_{4^n} and Sq_{4^n}. To illustrate Theorem 6.10, we compute the first 24 eigenmodes for T_1, T_4, T_{16} and Sq_1, Sq_4, Sq_{16} by using the Finite Element Libraray MÉLINA [Melina]. These computations are available on [BV]. Table 2 gives the numerical eigenvalues for these domains. Figures 16 and 17 represent some eigenfunctions and their corresponding nodal domains.

We notice that that fourth eigenfunctions on T_4 and Sq_4 are Courant-sharp and then we have

$$\mathfrak{L}_4(T_4) = \lambda_4(T_4) = \lambda_1(T_1) \quad \text{and} \quad \mathfrak{L}_4(Sq_4) = \lambda_4(Sq_4) = \lambda_1(Sq_1).$$

k	$\lambda_k(T_1)$	$\lambda_k(T_4)$	$\lambda_k(T_{16})$	$\lambda_k(Sq_1)$	$\lambda_k(Sq_4)$	$\lambda_k(Sq_{16})$
1	**22.7929**	5.6982	1.4246	**19.7392**	4.9348	1.2337
2	53.1834	13.2958	3.3240	49.3480	12.3370	3.0843
3	53.1834	13.2958	3.3240	49.3480	12.3370	3.0843
4	91.1715	**22.7929**	5.6982	78.9568	**19.7392**	4.9348
5	98.7692	24.6923	6.1731	98.6960	24.6740	6.1685
6	98.7692	24.6923	6.1731	98.6960	24.6740	6.1685
7	144.3549	36.0887	9.0222	128.3049	32.0762	8.0191
8	144.3549	36.0887	9.0222	128.3049	32.0762	8.0191
9	159.5502	39.8875	9.9719	167.7833	41.9458	10.4865
10	159.5502	39.8875	9.9719	167.7833	41.9458	10.4865
11	205.1360	51.2840	12.8210	177.6530	44.4132	11.1033
12	212.7336	53.1834	13.2959	197.3921	49.3480	12.3370
13	212.7336	53.1834	13.2959	197.3921	49.3480	12.3370
14	235.5265	58.8816	14.7204	246.7401	61.6850	15.4213
15	235.5265	58.8816	14.7204	246.7401	61.6850	15.4213
16	281.1122	70.2781	**17.5695**	256.6097	64.1524	**16.0381**
17	281.1123	70.2781	17.5695	256.6097	64.1524	16.0381
18	296.3075	74.0769	18.5192	286.2185	71.5546	17.8887
19	296.3075	74.0769	18.5192	286.2185	71.5546	17.8887
20	326.6980	81.6745	20.4186	315.8273	78.9568	**19.7392**
21	326.6980	81.6745	20.4186	335.5666	83.8916	20.9729
22	364.6862	91.1715	**22.7929**	335.5666	83.8916	20.9729
23	372.2838	93.0709	23.2677	365.1754	91.2938	22.8235
24	372.2838	93.0709	23.2677	365.1754	91.2938	22.8235

Table 2: Numerical eigenvalues of T_1, T_4, T_{16} and Sq_1, Sq_4, Sq_{16}.

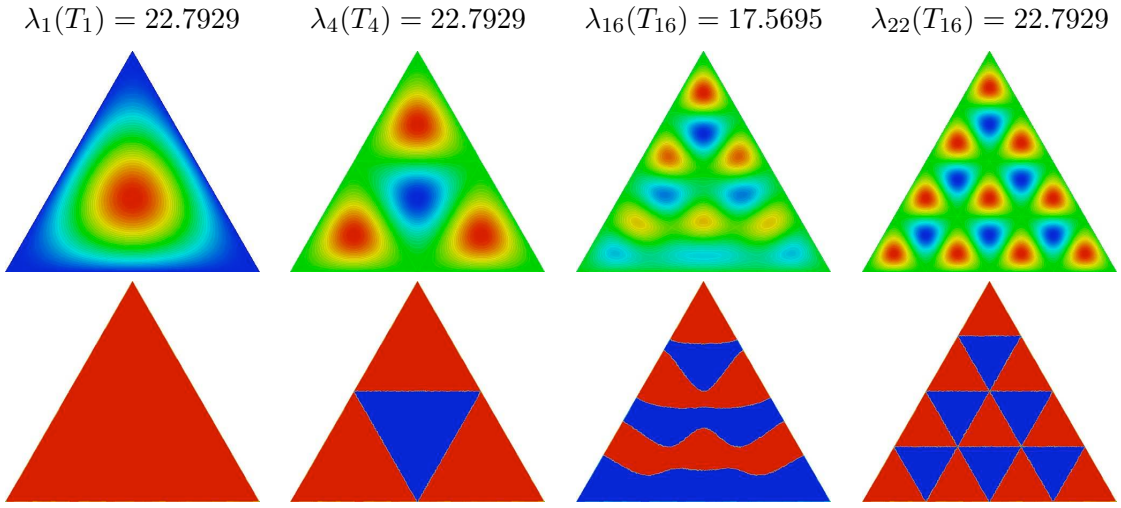

Figure 16: Eigenfunctions associated with $\lambda_1(T_1)$, $\lambda_4(T_4)$, $\lambda_{16}(T_{16})$, $\lambda_{22}(T_{16})$. *Top: eigenvalues, Middle: eigenfunctions, Bottom: the associated nodal domains.*

If the self-similar tiling associated with T_1 or Sq_1 is minimal, then we would have

$$\lambda_{16}(T_{16}) = \lambda_1(T_1) \quad \text{and} \quad \lambda_{16}(Sq_{16}) = \lambda_1(Sq_1).$$

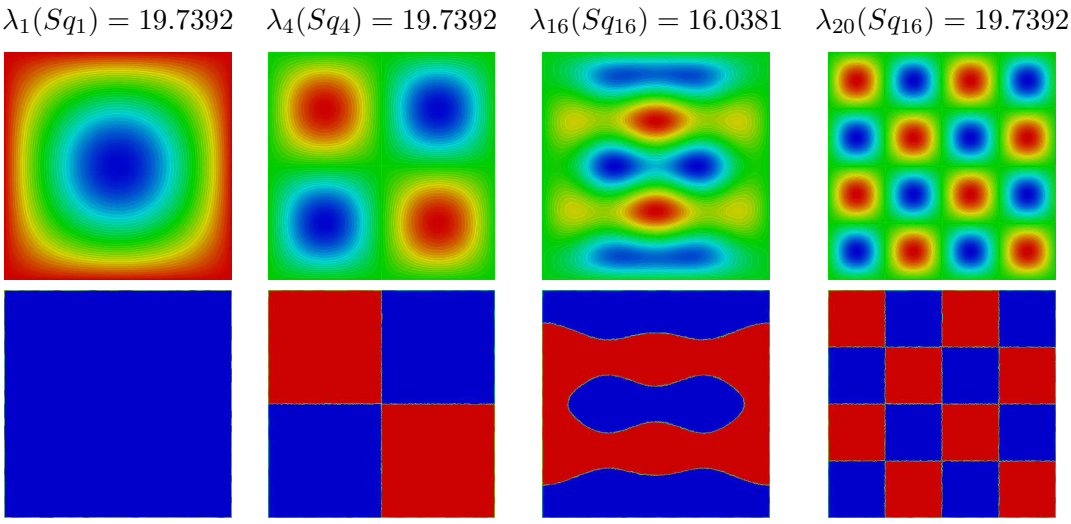

Figure 17: Eigenfunctions associated with $\lambda_1(Sq_1)$, $\lambda_4(Sq_4)$, $\lambda_{16}(Sq_{16})$, $\lambda_{20}(Sq_{16})$. *Top: eigenvalues, Middle: eigenfunctions, Bottom: the associated nodal domains.*

We observe that the 16-th eigenvalues on T_{16} and Sq_{16} are strictly less than $\lambda_1(T_1)$ and $\lambda_1(Sq_1)$. This is in agreement with Theorem 6.10. If we look at the following eigenfunctions, we see that $\lambda_{22}(T_{16}) = \lambda_1(T_1)$ and the 22-th eigenfunction on T_{16} has 16 nodal domains. For the square, the same situation appears for the 20-th eigenmode of Sq_{16}.

Let us mention that for the square, the eigenmodes are explicit. The eigenvalues of a square of side a are given by

$$\mu_{j,k} = \frac{\pi^2}{a^2}(j^2 + k^2), \quad j \geq 1,\ k \geq 1.$$

This formula can confirm the accuracy of the computations given in Table 2: the error is less than 10^{-4}. The 16-th eigenvalue on Sq_{16} is double and equals $13\pi^2/8$. Any linear combination of $(x, y) \mapsto \sin(5\pi x)\sin(\pi y)$ and $(x, y) \mapsto \sin(\pi x)\sin(5\pi y)$ is an eigenfunction for $\lambda_{16}(Sq_{16})$. In the case of the triangle, we do not have any explicit formula. Nevertheless, the computations show some multiple eigenvalues: in Table 2, each pair of numerically-close eigenvalues effectively corresponds to a double eigenvalue since the nodal sets of the associated eigenfunctions do not satisfy the symmetry properties of the domain. Indeed, if one eigenvalue is simple, the new eigenfunction obtained after symmetry is colinear with the considered eigenfunction. For example, the values λ_{16} and λ_{17}, given in Table 2, are numerically close and Figures 16 and 17 show that the eigenfunction associated with λ_{16} does not satisfy the symmetry property, so the eigenvalue λ_{16} is double.

7 Simulations on hexagons

7.1 Playing with hexagons

In order to explore the previous conjectures, we have to check the weaker following conjecture.

Conjecture 7.1
For given $k \in \mathbb{N}$, we consider the family of the open connected sets $\mathcal{H}^{(k)}$ which are union

of k hexagons of area 1. Then

$$\forall \Omega \in \mathcal{H}^{(k)}, \mathfrak{L}_k(\Omega) = \lambda_1(Hexa_1). \tag{43}$$

In other words, the k-partition of Ω by its constitutive hexagons is minimal over all k-partitions.

Remark 7.2
As shown in Subsection 6.5, this is wrong for triangles and squares (see Figures 16 and 17).

We explore this question by analyzing if weaker consequences of this conjecture are true. For example, Corollary 4.4 can be rephrased as follows.

Proposition 7.3
If the 'canonical' k-partition by hexagons is minimal, then for any extracted open set, the k-th eigenvalue of the Dirichlet Laplacian should be $\lambda_1(Hexa_1)$.

The partition of $\Omega \in \mathcal{H}^{(k)}$ by its hexagons is in general not bipartite but, as we have described previously, we can make it bipartite by considering $\Omega \backslash \cup_{j\in\sigma}\sigma_j$ where σ_j is one side of the constitutive hexagons. Of course, this procedure is not unique so we can associate to Ω a family of such 'cutted' open sets with cracks. Note that when the cutted set is no more connected, one can reinterpret the result as the direct sum of two independent spectral problems.

7.2 3-hexagons

- 3-hexagons without inside Dirichlet conditions, denoted by H_0^3.

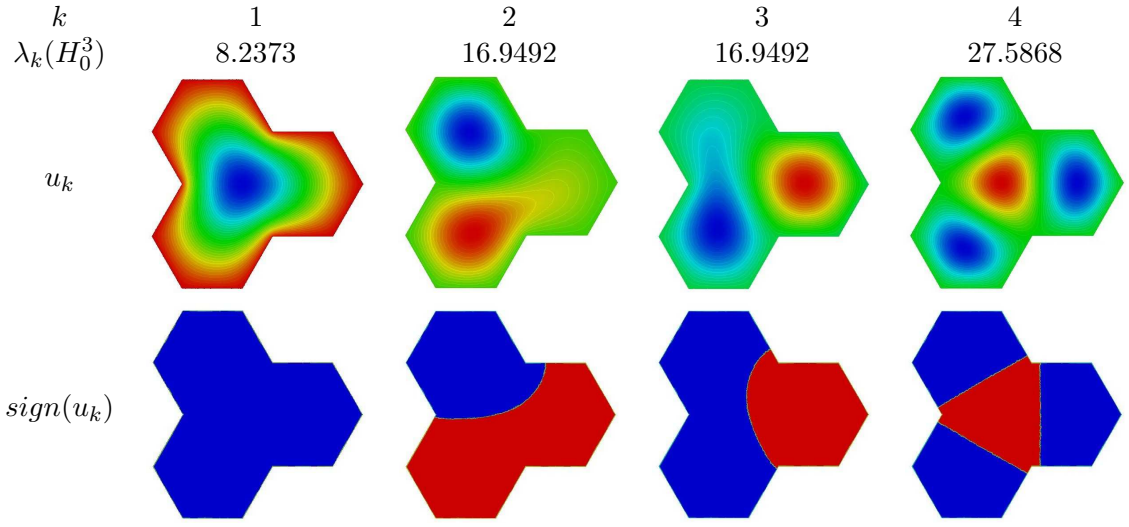

Figure 18: First four eigenmodes on 3-hexagons H_0^3.

Numerical eigenpairs are given in Figure 18 and we deduce

$$\mathfrak{L}_1(H_0^3) = \lambda_1(H_0^3), \qquad \mathfrak{L}_2(H_0^3) = \lambda_2(H_0^3) = \lambda_3(H_0^3),$$
$$\mathfrak{L}_3(H_0^3) < \lambda_4(H_0^3), \qquad \mathfrak{L}_4(H_0^3) = \lambda_4(H_0^3).$$

- Cracked 3-hexagons H_1^3.
  The domain H_1^3 is obtained from H_0^3 by removing the interior horizontal side of the constitutive hexagons. It is clear that

$$\mathfrak{L}_3(H_0^3) \leq \mathfrak{L}_3(H_1^3) = \lambda_3(H_1^3) = \lambda_1(Hexa_1).$$

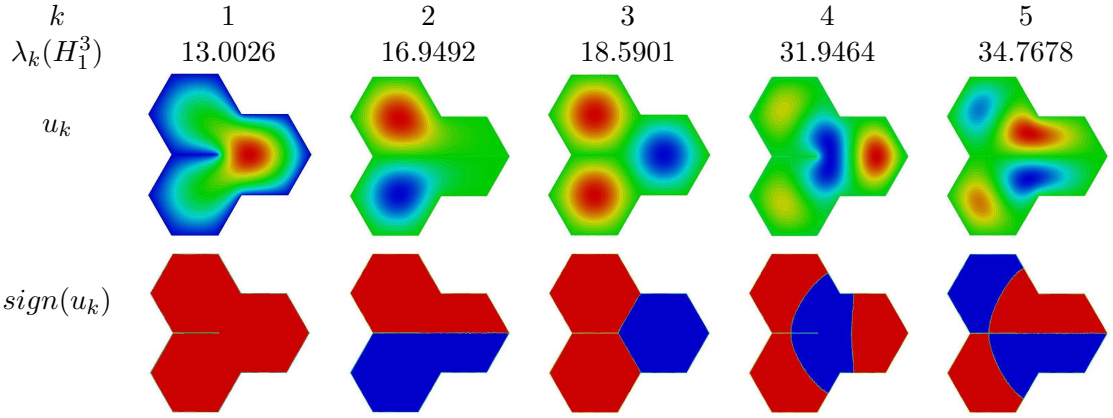

Figure 19: First five eigenmodes on cracked 3-hexagons H_1^3.

7.3 7-hexagons

Let H_0^7 be a ring of 6 patterns $Hexa_1$ at which we add the middle pattern $Hexa_1$ (see Figure 20). We construct new domains by removing some side of the constitutive hexagons to make the domain bipartite. After a possible symmetry, we can construct exactly 12 domains denoted by H_k^7, $k = 1, \ldots, 12$ and drawn in Figures 21.

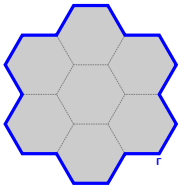

Figure 20: Domain with 7-hexagons H_0^7

We check that for any cracked 7-hexagons

$$\mathfrak{L}_7(H_0^7) \leq \mathfrak{L}_7(H_k^7) = \lambda_7(H_k^7) = \lambda_1(Hexa_1), \quad \text{for } k = 1, \ldots, 12.$$

Numerical eigenvalues are given in Table 3 for any domain H_k^7, $k = 0, \ldots, 12$. Figure 22 gives the first seven eigenfunctions on H_2^7. More simulations are available on [BV]. Numerical computations confirm Conjecture 7.1. For $k = 4, 5, 7, 9, 10$, the domain H_k^7 is not connected. Consequently, we notice that $\lambda_1(Hexa_1)$ arises before rank 7.

We emphasize that this does not work in the same way as for the triangle, because we have not self-similarity.

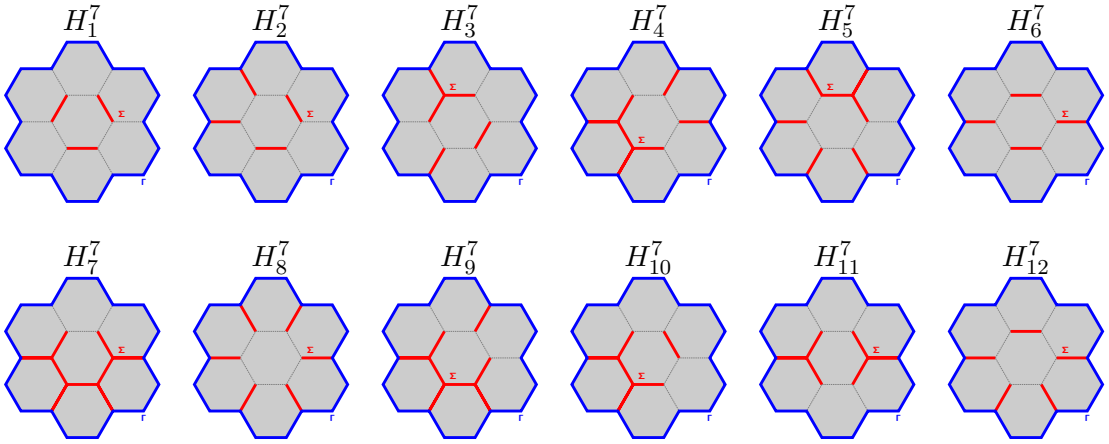

Figure 21: Every bipartite configurations from 7-hexagons

k	1	2	3	4	5	6	7
$\lambda_k(H_0^7)$	2.9369	7.3544	7.3544	12.8445	12.8445	14.8399	17.2250
$\lambda_k(H_1^7)$	10.3618	12.1236	12.1243	15.3192	15.7805	15.7807	**18.5901**
$\lambda_k(H_2^7)$	10.0981	12.4465	13.1570	14.6843	16.4286	17.1945	**18.5901**
$\lambda_k(H_3^7)$	10.7378	12.4433	13.6945	15.4251	16.7543	17.9174	**18.5901**
$\lambda_k(H_4^7)$	10.9022	13.4143	14.9745	17.5542	17.8478	**18.5901**	**18.5901**
$\lambda_k(H_5^7)$	10.3645	13.7750	16.3271	17.0038	17.7148	**18.5901**	**18.5901**
$\lambda_k(H_6^7)$	10.2306	12.9114	13.4639	14.5699	14.7908	17.6557	**18.5901**
$\lambda_k(H_7^7)$	11.5774	16.4434	17.0532	**18.5901**	**18.5901**	**18.5901**	**18.5901**
$\lambda_k(H_8^7)$	8.7087	15.4547	15.4555	16.9274	16.9276	17.2250	**18.5901**
$\lambda_k(H_9^7)$	11.6285	13.7275	16.2064	17.9874	**18.5901**	**18.5901**	**18.5901**
$\lambda_k(H_{10}^7)$	10.9273	12.2217	15.4757	16.3846	17.2592	**18.5901**	**18.5901**
$\lambda_k(H_{11}^7)$	11.2150	11.9100	16.3892	16.4434	16.4437	18.0900	**18.5901**
$\lambda_k(H_{12}^7)$	9.4695	13.2805	13.8475	16.3596	16.8214	17.3567	**18.5901**

Table 3: First seven smallest eigenvalues for every configurations of 7-hexagons.

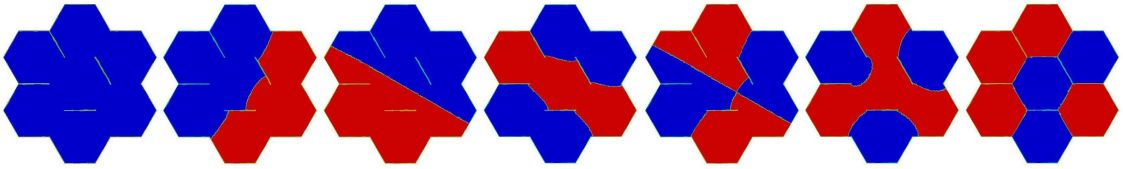

Figure 22: Nodal sets of the first seven eigenfunctions on H_2^7.

References

[AHHO] A. Ancona, B. Helffer and T. Hoffmann-Ostenhof. Nodal domain theorems à la Courant. Documenta Mathematica Vol. 9, p. 283-299 (2004).

[Al] G. Alessandrini. Nodal lines of eigenfunctions of the fixed membrane problem in general convex domains. Comment. Math. Helv., 69 (1), p. 142-154 (1994).

[BV] V. Bonnaillie-Noël and G. Vial. Computations for nodal domains and spectral minimal partitions.
http://www.bretagne.ens-cachan.fr/math/simulations/MinimalPartitions (2007).

[BBH] D. Bucur, G. Buttazzo, and A. Henrot. Existence results for some optimal partition problems. Adv. Math. Sci. Appl. 8 (2), p. 571-579 (1998).

[CTV1] M. Conti, S. Terracini and G. Verzini. An optimal partition problem related to nonlinear eigenvalues. Journal of Funct. Anal. 198, p. 160-196 (2003).

[CTV2] M. Conti, S. Terracini and G. Verzini. A variational problem for the spatial segregation of reaction-diffusion systems. Indiana Univ. Math. J. 54 (3), p. 779-815 (2005).

[CTV3] M. Conti, S. Terracini and G. Verzini. On a class of optimal partition problems related to the Fucik spectrum and to the monotonicity formula. Calc. Var. 22, p. 45-72 (2005).

[Hel] B. Helffer. Domaines nodaux et partitions spectrales minimales (d'après B. Helffer, T. Hoffmann-Ostenhof et S. Terracini). Séminaire EDP de l'Ecole Polytechnique. Déc. 2006.

[HHO1] B. Helffer and T. Hoffmann-Ostenhof. Converse spectral problems for nodal domains. To appear in Moscow Mathematical Journal (2007).

[HHO2] B. Helffer and T. Hoffmann-Ostenhof. On minimal partitions for the disk and the annulus. Provisory notes in February 2007.

[HHOT] B. Helffer, T. Hoffmann-Ostenhof and S. Terracini. Nodal domains and spectral minimal partitions. Preprint Nov. 2006.

[KiTr] R. Kiwan and M. Traizet. Problème isopérimétrique pour les pavages du plan. Preprint 2007.

[Lan] N. Landais. Problèmes de régularité en optimisation de forme. Thèse de doctorat, ENS Cachan Bretagne (2007).

[Melina] D. Martin. The finite element library Mélina.
http://perso.univ-rennes1.fr/daniel.martin/melina (2005).

[Mel] A. Melas. On the nodal line of the second eigenfunction of the Laplacian on $\mathbb{R}^2$. J. Differential Geom. 35, p. 255-263 (1992).

[Pl] A. Pleijel. Remarks on Courant's nodal theorem. Comm. Pure. Appl. Math., 9, p. 543-550 (1956).